

Development of New Conveyer Directly Driven by Contact-less Energy Transmission System

Hyung-Beom Park · Han-Seok Park* · Kyung-II Woo

Abstract

This paper focuses on development of new conveyer directly driven by the contact-less energy transmission system. The effect of the resonant circuit and the flux linkage characteristics caused from that are analyzed by using 3D finite element analysis. From the result it is shown that the resonant circuit needs to transfer energy from the primary core to the secondary core. Also the influence of the linear induction motor on the contact-less energy transmission system is presented. New conveyer and the experimental apparatus was manufactured by using the contact-less energy transmission system and the linear induction motor. Possibility of realization of the conveyer is proved by comparison the simulation result which is obtained by using 2D finite element analysis with experimental one and the characteristic of the voltage and resonant current.

Key Words : Contact-Less Energy Transmission System, Conveyer, Finite Element Analysis, Linear Induction Motor, Resonant Circuit

1. Introduction

In the last ten years, a new energy transmission system, contact-less energy transmission system (CETS), has been developed and now thousands of these kinds of devices using this technology are working all around[1-6]. The transformer used in the CETS stretches the primary winding into a long loop and places the secondary winding on an open-end core surrounds the primary conductors

and allows relative movement between the two windings. The reduced coupling of the open core geometry is compensated by a higher primary frequency. So the CETS has a resonant circuit.

This paper focuses on development of new conveyer directly driven by the CETS. The linear induction motor is used to generate a linear motion. The effect of the resonant circuit and the flux linkage characteristics caused from that are analyzed by the 3D finite element analysis. Also the influence of the linear induction motor on the CETS is presented. The experimental apparatus was manufactured and the simulation result and the experimental one obtained through the speed control of the linear induction motor are compared.

* Main author : Professor in the Division of
Electrical, Control Engineering of
Pukyong National University
Tel : +82-51-629-6315, Fax : +82-51-629-6305
E-mail : phanseok@pknu.ac.kr
Date of submit : 2008. 11. 11
First assessment : 2008. 11. 13
Completion of assessment : 2008. 12. 9

Because the computation time by using 3D finite element analysis is very long 2D finite element analysis is used to simulate the speed control of the linear induction motor. From this comparison we knew realization possibility of new conveyer.

2. Finite element Analysis

2.1 Analysis model

Fig. 1 shows the CETS model with an alternative switching for the primary source adopted in this paper. There are one primary core and two secondary cores. Each secondary core can be used as CETS, that is, there are two CETSs. The lamination depths of the primary and the secondary core are 300 [mm] and 60 [mm], respectively. The air gap length is 0.5 [mm]. The number of turns of coil is 45 and the secondary is 100. The material type of the primary and secondary core is S45C. In Fig. 2 (b) the side A of the primary coil and core are segmented to reduce the leakage flux. In this figure, the dotted square box is the secondary core. Fig. 2 shows the 3D structure of CETS with the linear induction motor. In this figure, we consider the left CETS only. The linear induction motor is 3 phase, 4 poles and the rated input voltage is 220[V].

2.2 Governing equation

The fundamental equation of the magnetic field using 3D FEM with edge element can be written using the magnetic vector potential as follows:

$$\text{rot}(\nu \text{rot}A) = J_0 + J_e \tag{1}$$

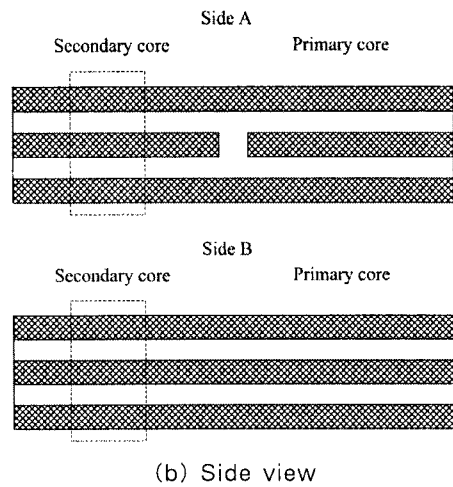
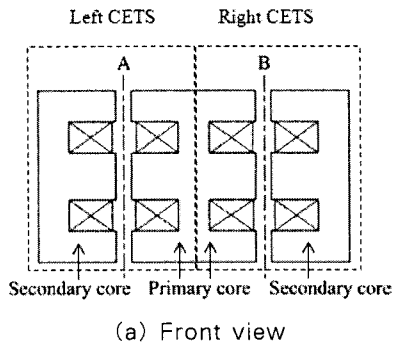


Fig. 1. Analysis model

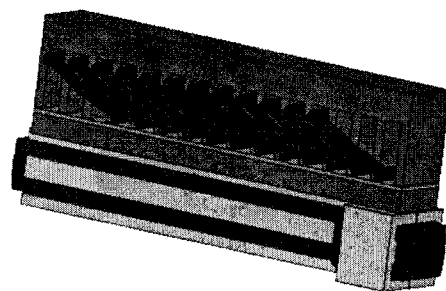


Fig. 2. 3D structure of CETS with the linear induction motor

where ν is the reluctivity, J_0 is the current density and J_e is the eddy current density. J_e is given as follows:

$$J_e = -\sigma \left(\frac{\partial A}{\partial t} + \nabla \Phi \right) \quad (2)$$

where σ is the electrical conductivity and Φ is the electric scalar potential.

From (2) and $J_e = 0$, we can obtain the following equation.

$$\nabla \cdot \left\{ -\sigma \left(\frac{\partial A}{\partial t} + \nabla \Phi \right) \right\} = 0 \quad (3)$$

The magnetic field can be calculated by coupling (1)–(3).

The following equations can be obtained by the Galerkin's method from (1) and (3).

$$\begin{aligned} G_i &= \int_V \text{rot } N_i \cdot (v \text{ rot } A) dV - \int_{V_e} N_i \cdot J_0 dV \\ &+ \int_{V_e} N_i \cdot \left\{ \sigma \left(\frac{\partial A}{\partial t} + \nabla \Phi \right) \right\} dV \\ &- \int_S N_i \cdot \{ (v \text{ rot } A) \times n \} dS = 0 \end{aligned} \quad (4)$$

$$\begin{aligned} G_{ii} &= \int_{V_e} \nabla N_i \cdot \sigma \left(\frac{\partial A}{\partial t} + \nabla \Phi \right) dV \\ &+ \int_{S_e} N_i \cdot \left\{ -\sigma \left(\frac{\partial A}{\partial t} + \nabla \Phi \right) \right\} \cdot n dS = 0 \end{aligned} \quad (5)$$

where N_i is the vector interpolation function for A , N_i is the scalar interpolation function for Φ , V is the analyzed region, V_e is the region of the conductor with the eddy current, S and S_e are the boundary of analyzed region and eddy current region, respectively. n is the unit outward normal vector on the surface S and S_e . The 3D region is divided into tetrahedral elements, and the matrix of the FEM is solved by the CG method and

Newton-Rahpson iteration technique is used for the non-linear characteristics.

The circuit equations (6) and (7) should be considered to solve (4) and (5).

$$[U] = [R][I] + [L_0] \frac{d}{dt} [I] + [E] \quad (6)$$

$$[E] = \frac{d}{dt} [\lambda_s] \quad (7)$$

where,

$[U] = (U_a)$: phase voltages,

$[I] = (i_a)$: phase currents,

$[R] = (R_a)$: primary winding resistances,

$[L_0] = (L_a)$: end winding leakage inductances,

$[E] = (E_a)$: phase e.m.f.

$[\lambda_s] = (\lambda_a)$: phase flux linkages.

3. Characteristics analysis and experiment

3.1 Effect of resonant circuit

The resonant circuit should be used to reduce the effect of the leakage flux in CETS. Fig. 3 shows the electrical scheme of CETS to check the effectiveness of the resonant capacitances. In this figure, the primary series capacitor has been introduced to compensate the very high leakage inductance of the primary and the secondary coils. It is possible to calculate this capacitor from the condition of running at resonance by (8).

$$C_p = 1 / \left(4\pi^2 f^2 (L_{1s} + L_{2s}') \right) \quad (8)$$

where L_{1s} is the leakage inductance of the

primary, L_{2s}' is the referred secondary leakage inductance to the primary.

The secondary parallel capacitor, mounted in the secondary side, compensates the magnetizing inductance. Its value can be also calculated from resonant condition of secondary circuit by (9).

$$C_s = 1 / (4\pi^2 f^2 L_m'') \tag{9}$$

where L_m'' is the referred magnetizing inductance to the secondary.

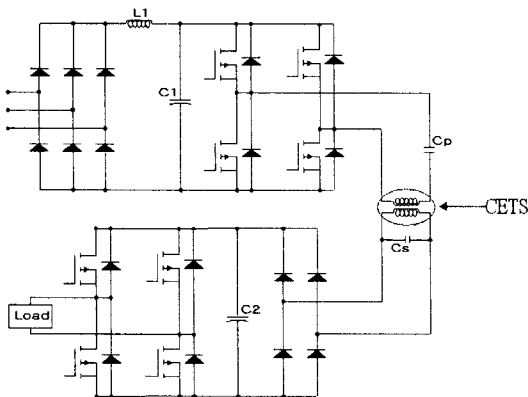


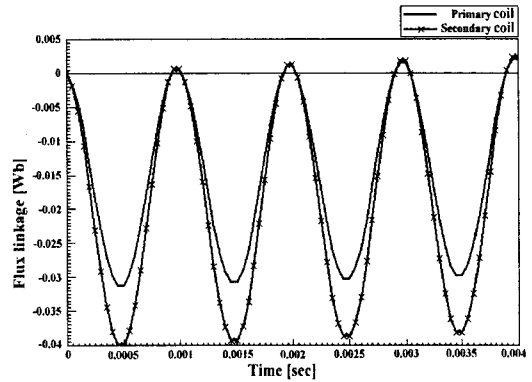
Fig. 3. Electrical scheme of CETS

Fig. 4 (a) and (b) show the primary and secondary coil flux linkage characteristics when the resonant circuit is considered or not. From this figure it is shown that the resonant circuit needs to transfer energy from the primary core to the secondary core.

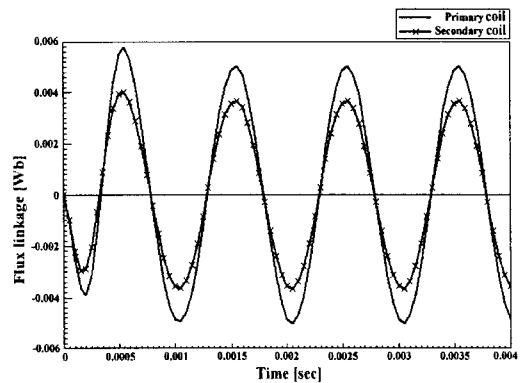
3.2 Dynamic characteristics

To drive the linear induction motor the 6 step inverter is used. In Fig. 5, the arrow type flux line is shown when the linear induction motor begins to start. From this figure it is known that the magnetic flux could affect the characteristic of the

CETS. Therefore the protection of the CETS from the linear induction motor should be done to obtain the exact behavior characteristics.



(a) Not considering the resonant circuit



(b) Considering the resonant circuit

Fig. 4. Coil flux linkage characteristics

3.3 Experimental results

Fig. 6 shows the front view of the simplified design model. In this system the four secondary cores are used at front and back sides. They are used to supply the power to the linear induction motor. Every secondary core could be used to drive the other different systems. Fig. 7 is the manufactured system. Fig. 8 shows the experimental results. In this figure, the DC link voltage and the resonant current of the primary

core are 308[V] and 6[A], respectively. At the first fluctuating position of the current the linear induction motor begins to start.

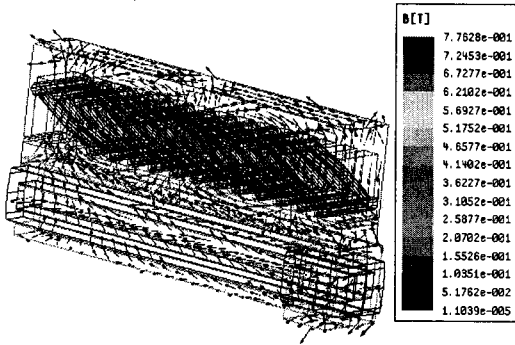


Fig. 5. Flux line characteristic

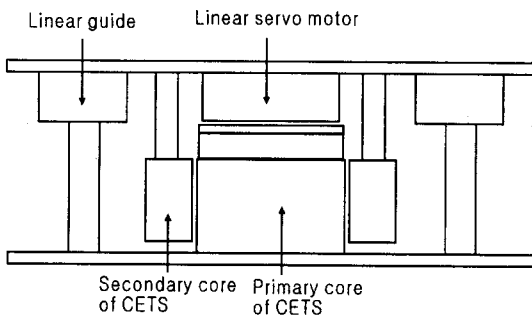


Fig. 6. Front view of simplified design model

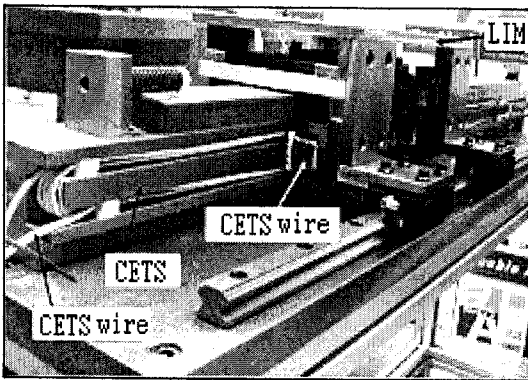


Fig. 7. Manufactured system

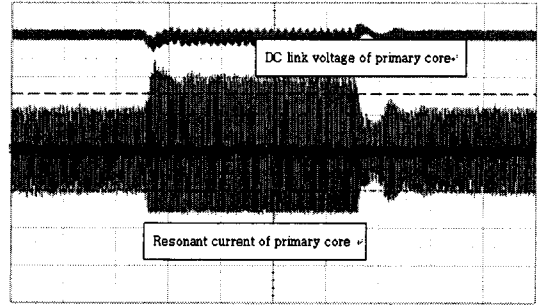
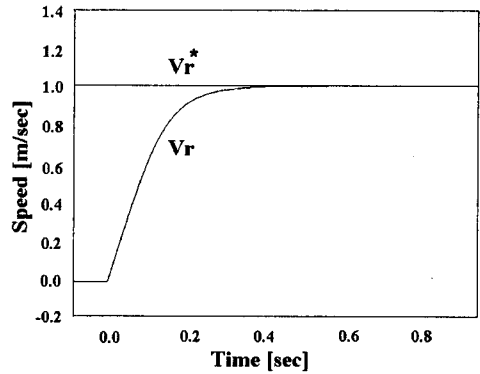
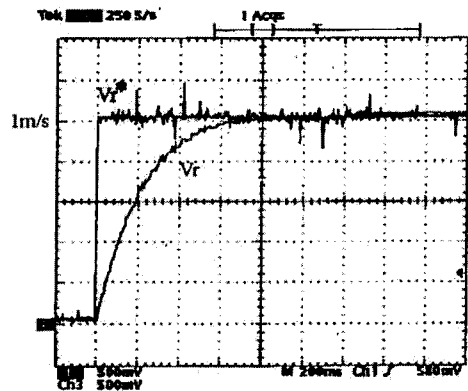


Fig. 8. Voltage and resonant current characteristics (ch1: inverter DC link(100V/div), CH2: resonant current(10A/div))



(a) Simulation



(b) Experiment

Fig. 9. Speed control characteristic

Fig. 9 (a) and (b) are the simulation and experimental ones obtained from the speed control of the linear induction motor respectively. Because

the computation time by using 3D finite element analysis is very long 2D finite element analysis was used to simulate the speed control of the linear induction motor. A reference speed is 1 [m/sec]. It is known that the simulated speed converges on the reference speed a little faster than experiment. The difference might be caused from the influence of the magnetic flux of the linear induction motor on the CETS. From this figure we know that realization of new conveyer is possible.

3. Conclusion

This paper focuses on development of new conveyer directly driven by the CETS. From the simulation result of flux linkage characteristics it is shown that the resonant circuit needs to transfer energy from the primary core to the secondary core. Also because the magnetic flux density could affect the characteristic of the CETS the protection of the CETS from the linear induction motor should be done to obtain the exact behavior characteristics. From the simulation result and experimental one obtained from the speed control of the linear induction motor we knew realization possibility of new conveyer.

Acknowledgement

This work was supported by the Pukyong National University Research Fund in 2006 (PK-2006-050)

References

- [1] Jacobus M. Barnard, Jan A. Ferreria, Jacobus Daniel van Wyk, "Sliding Transformer for Linear Contactless Power Delivery", IEEE Transaction on Industrial Electronics, Vol. 44, No. 6, December 1997.
- [2] Dae-Hyun Koo, Pyo-Jung Hong, Yun-Hyun Cho, Koon-Seok Chung, "Design and Simulation of a Contactless Power Transimission System", Automotive Electrical Equipment Optimization of Electronic Equipment, pp. 377-382, Brasov, 2002.
- [3] D. A. G. Pedder, A. D. Brown and J. A. Skinner, "A Contactless Electrical Energy Transmission System ", IEEE Trans.on Industrial Electronics, Vol. 46, No. 1, pp. 23-30, 1999.
- [4] J. M. Barnard, J. A. Ferreria, J. D. van Wyk, "Optimizing sliding transformers for contactless power transmission systems", IEEE PESC, Vol. 1, pp. 245-251, June 1995.
- [5] Junji Hirai, Tae-Woong Kim, Atsuo Kawamura, "Study on Crosstalk in Inductive Transmission od Power and Information", IEEE Transactions on Industry Electronics, Vol. 46, No. 6, PP. 1174-1182, Dec. 1999.
- [6] Kyung il Woo, Han-Seok Park, Hyeong-Beom Park, "3D Finite Element Analysis of Contact-less Power Supply with Linear Servo Motor", Journal of the Korean Society of Marine Engineering, Vol. 31, No. 2, pp. 190-196, Mar. 2007.

Biography

Hyung-Beom Park

He received B.S. and M.S. degrees in Electrical Engineering from Pukyong National University. He is currently in the Ph.D. course in Electrical Engineering from Pukyong National University. He is a managing director of the JUWON Engineering.

Han-Seok Park

He received the B.S. and M.S. degrees in Electrical Engineering from Chung Ang University. He received the Ph.D. degree in Electrical Engineering from Korea Maritime University. He is currently a professor in the Division of Electrical, Control and Instrument Engineering of Pukyong National University. His research interest are energy conversion system and substitute energy system.

Kyung-II Woo

He received the B.S, M.S., and Ph. D. degrees in Electrical Engineering from Hanyang University. He is currently a associate professor in the Division of Electrical, Control and Instrument Engineering of Pukyong National University. His research interests are numerical analysis of electrical machines and control.